$^{13}C-^{13}C$ and $^{15}N-^{13}C$ correlation spectroscopy of membrane-associated and uniformly labeled human immunodeficiency virus and influenza fusion peptides: Amino acid-type assignments and evidence for multiple conformations

Michele L. Bodner,[1] Charles M. Gabrys,[1] Jochem O. Struppe,[2] and David P. Weliky[1,a)]
[1]*Department of Chemistry, Michigan State University, East Lansing, Michigan 48824, USA*
[2]*Bruker Biospin Corporation, NMR Division, Billerica, Massachusetts 01821, USA*

(Received 29 October 2007; accepted 6 December 2007; published online 4 February 2008)

Many viruses which cause disease including human immunodeficiency virus (HIV) and influenza are "enveloped" by a membrane and infection of a host cell begins with joining or "fusion" of the viral and target cell membranes. Fusion is catalyzed by viral proteins in the viral membrane. For HIV and for the influenza virus, these fusion proteins contain an ~20-residue apolar "fusion peptide" that binds to target cell membranes and plays a critical role in fusion. For this study, the HIV fusion peptide (HFP) and influenza virus fusion peptide (IFP) were chemically synthesized with uniform ^{13}C, ^{15}N labeling over large contiguous regions of amino acids. Two-dimensional $^{13}C-^{13}C$ and $^{15}N-^{13}C$ spectra were obtained for the membrane-bound fusion peptides and an amino acid-type ^{13}C assignment was obtained for the labeled residues in HFP and IFP. The membrane used for the HFP sample had a lipid headgroup and cholesterol composition comparable to that of host cells of the virus, and the ^{13}C chemical shifts were more consistent with β strand conformation than with helical conformation. The membrane used for the IFP sample did not contain cholesterol, and the chemical shifts of the dominant peaks were more consistent with helical conformation than with β strand conformation. There were additional peaks in the IFP spectrum whose shifts were not consistent with helical conformation. An unambiguous ^{13}C and ^{15}N assignment was obtained in an HFP sample with more selective labeling, and two shifts were identified for the Leu-9 CO, Gly-10 N, and Gly-10 Cα nuclei. These sets of two shifts may indicate two β strand registries such as parallel and antiparallel. Although most spectra were obtained on a 9.4 T instrument, one $^{13}C-^{13}C$ correlation spectrum was obtained on a 16.4 T instrument and was better resolved than the comparable 9.4 T spectrum. More selective labeling and higher field may, therefore, be approaches to obtaining unambiguous assignments for membrane-associated fusion peptides. © *2008 American Institute of Physics*. [DOI: 10.1063/1.2829984]

INTRODUCTION

Enveloped viruses such as human immunodeficiency virus (HIV) and influenza virus are surrounded by a membrane and infection of target cells begins with fusion, i.e., the joining of the viral and target cell membranes into a single membrane. After fusion, the viral nucleocapsid is inside the target cell and can initiate viral replication. HIV fuses directly with the plasma membrane of the cell whereas influenza is first endocytosed into the target cell and fusion occurs between the viral and endosomal membranes.[1,2] Understanding viral fusion is important because fusion is a key step in the viral life cycle and because fusion is a target for antiviral therapeutics.

There is a high kinetic barrier to membrane fusion and both the HIV and the influenza virus have fusion proteins in the viral membrane which catalyze fusion. The fusion proteins of both viruses contain a N-terminal "fusion peptide" (FP) which plays a critical role in fusion.[3,4] The HIV FP is an ~20-residue apolar domain at the N-terminus of the gp41 fusion protein and the influenza FP is an analogous domain at the N-terminus of the HA2 subunit of the hemagglutinin fusion protein. The sequences are different for the FPs of the two viruses. The FP is hidden within the fusion protein until a conformational change is triggered which exposes the FP and allows it to interact with the membrane of the target cell.[5–9] The triggering event for influenza virus is the reduction of the endosomal *p*H to ~5, while for HIV the event is viral protein binding to target cell receptors.[10]

This paper focuses on HIV and influenza viral FPs in the absence of the remaining fusion proteins. These peptides serve as good model systems for understanding some aspects of viral fusion as evidenced by their ability to catalyze fusion between lipid vesicles and by mutational studies which show strong correlations between FP-induced fusion and viral/host cell fusion.[3,11]

There have been structural studies on the HIV FP (HFP) and the influenza FP (IFP) in a variety of environments using a wide array of biophysical techniques. In detergent micelles at peptide:detergent $\leqslant 0.01$, both IFP and HFP are mono-

a)Author to whom correspondence should be addressed. Tel.: 517-355-9715. FAX: 517-353-1793. Electronic mail: weliky@chemistry.msu.edu.

meric. The IFP structure in detergent at the fusogenic *p*H of 5 is a helix from residues 2–10, a turn from residues 11–14, and a helix from residues 15–18.[12–14] There is general agreement among liquid-state NMR studies that HFP in detergent contains a continuous helix over residues 4–12 and some studies suggest that the helix continues to residue 19.[15–19] For membrane-associated IFP and HFP, populations of helical and β strand conformations have been observed with helical conformation favored at lower peptide:lipid and in membranes lacking cholesterol and β strand conformation favored at higher peptide:lipid and in membranes containing cholesterol.[3,18,20–22] The membranes of host cells of HIV and influenza virus contain ~30 mol % cholesterol and the membranes of HIV and influenza virus contain ~45 mol % cholesterol.[23–26] Measurements of solid-state nuclear magnetic resonance (NMR) dipolar couplings between HFPs showed that the β strand structure is oligomeric and provided evidence for significant populations of parallel and antiparallel strand alignments.[27]

Solid-state NMR of peptides and proteins has often relied on selective ^{13}C and ^{15}N labeling to probe structure while more recent solid-state NMR has focused on solving three-dimensional structures of uniformly (U-) ^{13}C, ^{15}N labeled peptides and proteins in a manner analogous to liquid-state NMR techniques.[28–36] Studies of the microcrystalline 61-residue α-spectrin Src-homology (SH3) domain and the 76-residue microcrystalline protein ubiquitin are examples of the latter approach.[37–40] The protein was uniformly or extensively ^{13}C, ^{15}N labeled and a complete ^{13}C, ^{15}N assignment and three-dimensional (3D) structure were obtained from a combination of multidimensional $^{13}C-^{13}C$, $^{15}N-^{13}C$, and $^{15}N-^{15}N$ experiments. Another recent example is the 40-residue β-amyloid peptide in fibrillar form. The β-amyloid samples had "scatter uniform labeling" in which only one residue of each amino acid type was uniformly ^{13}C, ^{15}N labeled. A combination of two-dimensional (2D) $^{13}C-^{13}C$ and $^{15}N-^{13}C$ experiments was used for assignment and structure determination.[41–44]

One long-term aim of our research is development of high-resolution structural models of membrane-associated fusion peptides. It is likely that these models can be generated more quickly with peptides with more uniform labeling because relative to selective labeling, fewer samples will be required. However, unambiguous assignment is typically a prerequisite to high-resolution NMR structure determination, and spectral linewidths and dispersion play a large role in determining the number of uniformly labeled residues that can be unambiguously assigned. This is a key issue for membrane-associated fusion peptides because the ^{13}C linewidths of 2–3 ppm are significantly broader than the ~0.5 ppm linewidths of microcrystalline proteins. Another challenge in the analysis of spectra of membrane-associated fusion peptides is lower signal-to-noise ratio due both to broader linewidths and to the relatively small amount of peptide in the sample volume and the corresponding large amount of physiologically relevant lipids and water.

In the present work, these methodological questions were addressed by obtaining and assigning 2D $^{13}C-^{13}C$ and $^{15}N-^{13}C$ spectra of membrane-associated HFP and IFP samples with different numbers of uniformly labeled residues. The study was limited to two dimensions rather than more information-rich 3D spectra because each 2D spectrum required at least a few days signal averaging time and a 3D spectrum would require several times that duration.[39] One specific aim of this study was, therefore, assessment of the number of uniformly labeled residues that can be unambiguously assigned with 2D spectra. Although this work was focused on assignment and did not include any direct structural measurements, the assigned ^{13}C shifts were compared to ^{13}C shifts typical of helical or β strand conformations.[45] Relative to selectively labeled peptides or proteins, this type of empirical analysis is generally more conclusive in uniformly labeled samples for which there may be a large number of assigned chemical shifts in a contiguous sequence of residues that are consistent with either helical or with β strand conformation.

EXPERIMENTAL

Materials

Rink amide resin was purchased from Advanced Chemtech (Louisville, KY) and 9-fluorenylmethoxycarbonyl (FMOC)-amino acids were purchased from Peptides International (Louisville, KY). Isotopically labeled amino acids were purchased from Cambridge (Andover, MA) and were FMOC protected using literature procedures.[46,47] The lipids 1-palmitoyl-2-oleoyl-sn-glycero-3-phosphocholine (POPC), 1-palmitoyl-2-oleoyl-sn-glycero-3-[phospho-L-serine] (POPS), 1-palmitoyl-2-oleoyl-sn-glycero-3-phosphoethanolamine (POPE), 1-palmitoyl-2-oleoyl-sn-glycero-3-[phospho-rac-(1-glycerol)] (POPG), phosphatidylinositol (PI), and sphingomyelin were purchased from Avanti Polar Lipids, Inc. (Alabaster, AL). Most other reagents were obtained from Sigma (St. Louis, MO).

Fusion peptides

The HFP-U3 peptide (sequence *AVGIGALFLGFLGAAGSTMGARSKKK*) was synthesized with the 23 N-terminal residues of the LAV_{1a} strain of the HIV-1 gp41 fusion protein followed by three additional lysines for improved solubility. The underlined residues in the sequence had uniform ^{13}C, ^{15}N labeling. The HFP-U12 peptide (sequence *AVGIGALFLGFLGAAGSTMGARSCKKKKKKW*) was synthesized with the 23 N-terminal residues of the LAV_{1a} strain of the HIV-1 gp41 fusion protein followed by cysteine, lysine, and tryptophan residues. The cysteine would allow cross-linking of HFPs, the lysines increased solubility, and the tryptophan served as a 280 nm chromophore for peptide quantitation. In the present study, HFP-U12 was predominantly non-cross-linked as judged by monomeric molecular weight determined in analysis of analytical ultracentrifugation data.[48] The IFP-U10 peptide (sequence *GLFGAIAGFIENGWEGMIDGGGKKKK*) was synthesized with the 20 N-terminal residues of the HA2 domain of the X31 strain influenza hemagglutinin fusion protein followed by two glycines and four lysines for improved solubility.[49]

All peptides were synthesized as their C-terminal amides using a peptide synthesizer (ABI 431A, Foster City, CA) equipped with FMOC chemistry. Peptides were purified by reversed-phased high-performance liquid chromatography (HPLC) using a preparative C_{18} column (Vydac, Hesperia, CA) and a water/acetonitrile gradient containing 0.1% trifluoroacetic acid. Matrix assisted laser desorption ionization mass spectroscopy was used to confirm the identity of the peptides. HFP-U3 had uniform ^{13}C, ^{15}N labeling at Phe-8, Leu-9, and Gly-10, HFP-U12 had uniform ^{13}C, ^{15}N labeling over the 12 residues from Gly-5 to Gly-16, and IFP-U10 had uniform ^{13}C, ^{15}N labeling from Gly-1 to Ile-10.

Preparation of membrane-associated fusion peptides

HFP samples were prepared using an "LM3" lipid/cholesterol mixture reflecting the approximate lipid headgroup and cholesterol content of membranes of host cells infected by HIV.[24,26,50] This lipid mixture contained POPC, POPE, POPS, PI, sphingomyelin, and cholesterol in a 10:5:2:1:2:10 molar ratio. The IFP sample was prepared with a "PC/PG" mixture which contained a 4:1 molar ratio of POPC:POPG without cholesterol. This mixture was chosen because it has been used by other investigators studying IFP.[13,51] The PC/PG mixture has been a common model membrane choice for experiments above 0 °C because (1) the lipids are in the liquid-crystalline rather than the gel phase at temperatures greater than 0 °C; and (2) relative to the gel phase, the liquid-crystalline phase of pure lipids is considered to be more representative of the cell membrane.[52] In addition, the headgroups of the POPC and POPG lipids are neutral and negatively charged, respectively, and an ~4:1 ratio of neutral to negatively charged headgroups is typical of the membranes of many cell types.

Lipid and cholesterol powders were dissolved together in chloroform. The chloroform was removed under a stream of nitrogen followed by overnight vacuum pumping. Lipid dispersions were formed by addition of ~2 ml buffer followed by homogenization with ten freeze-thaw cycles. Large unilamellar vesicles (LUVs) were prepared by extruding the lipid dispersions ~30 times through two stacked polycarbonate filters with 100 nm diameter pores (Avestin, Inc., Ottawa, ON, Canada). An ~2 ml peptide solution was added to the LUV solution, stored overnight, and then centrifuged at ~100 000 g for 5 h to pellet the LUVs and associated bound peptide. Nearly all peptide bound to LUVs under these conditions and unbound peptide did not pellet.[50] The peptide/LUV pellet was transferred by a spatula to a 4 mm diameter magic angle spinning (MAS) NMR rotor with ~40 μl available sample volume.

The HFP-U3 and HFP-U12 samples contained 0.8 μmol peptide, 20 μmol total lipid, and 10 μmol cholesterol and the IFP-U10 sample contained 0.3 μmol peptide and 15 μmol total lipid. The HFP samples were made with a *p*H 7 buffer containing 5 mM *N*-2-hydroxyethylpiperazine-*N'*-2-ethanesulfonic acid (HEPES) and the IFP sample was made with a *p*H 5 buffer composed of 5 mM HEPES and 10 mM 2-(*N*-morpholino)ethanesulfonic acid. Both buffers contained 0.01% NaN_3 preservative. The selection of buffer *p*H was based on the *p*H of viral fusion and on the observation that the fusion activity of IFP is much higher at *p*H 5 than at *p*H 7.[49,53]

Synthesis of the setup compounds *N*-acetyl leucine and I4-U2 peptide

Uniformly labeled *N*-acetyl-leucine (U-NAL) served as a general setup compound for the solid-state NMR experiments. Synthesis began with addition of uniformly ^{13}C, ^{15}N labeled leucine (24.8 mg) to glacial acetic acid (0.5 ml) and heating/stirring at 100 °C. After the addition of 1-^{13}C-acetic anhydride (38 μl), the solution was cooled to 80 °C and water (1 ml) was added to react with any excess acetic anhydride. The U-NAL product was washed with cyclohexane and the cyclohexane was subsequently removed under vacuum. Residual solvents were removed with the following sequential steps: (1) Water aspirator vacuum until weight loss was no longer detected, (2) drying in a vacuum dessicator, and (3) dissolution in water followed by lyophilization.[54] Liquid-state NMR confirmed the U-NAL synthesis.

U-NAL (16.5 mg) and unlabeled NAL (89.4 mg, ICN, Aurora, OH) were dissolved in ~5 ml of water with gentle heating. After cooling, the solution was filtered through a 0.22 μm sterile syringe filter (Millipore, Bedford, MA). A microcrystalline solid was formed with slow evaporation of the water.

A lyophilized "I4-U2" peptide (sequence *AEAAAKEALAKEAAAKA*) was used as an additional setup compound for 2D $^{15}N-^{13}C$ correlation spectroscopy and was predominantly helical.[22,55] The peptide was synthesized and purified in a manner similar to the other peptides and contained uniform ^{13}C, ^{15}N labeling at Ala-8 and Leu-9.

NMR spectroscopy

Most NMR spectra were taken on a 9.4 T spectrometer (Varian Infinity Plus, Palo Alto, CA) using a MAS probe designed for a 4 mm diameter rotor. The ^{13}C detection channel was tuned to 100.8 MHz, the ^{1}H decoupling channel was tuned to 400.8 MHz, and for $^{15}N-^{13}C$ correlation experiments, the third channel was tuned to ^{15}N at 40.6 MHz. The ^{13}C chemical shifts were referenced to the methylene resonance of solid adamantane at 40.5 ppm and yielded ^{13}C shifts that were directly comparable to liquid-state ^{13}C shifts referenced according to IUPAC standards.[56] The ^{15}N frequency at 0 ppm was calculated by multiplying the ^{13}C frequency at 0 ppm by 0.402 979 946. This ^{15}N referencing was based on the ratio of ratios $(\gamma_N/\gamma_H)/(\gamma_C/\gamma_H)$ where γ_N, γ_H, and γ_C are the respective IUPAC gyromagnetic ratios for ^{15}N, ^{1}H, and ^{13}C.[57] The sample temperature was −50 °C, and the MAS frequency was 6800 ± 2 Hz for the 2D $^{13}C-^{13}C$ correlation experiments and 7000 ± 2 Hz for the 2D $^{15}N-^{13}C$ correlation experiments. Previous MAS NMR measurements on membrane-bound FP samples have shown a threefold improvement in ^{13}C sensitivity at −50 °C relative to room temperature and have also shown that shifts at selectively labeled sites and presumably local FP structure are very similar at the two temperatures.[58]

2D $^{13}C-^{13}C$ experimental details

The 2D $^{13}C-^{13}C$ correlation spectra at 9.4 T were obtained with a double resonance $^{1}H/^{13}C$ probe configuration because the ^{13}C signal-to-noise ratio is ~1.5 times higher than in the triple resonance $^{1}H/^{13}C/^{15}N$ configuration. Correlations were generated by the proton-driven spin diffusion (PDSD) pulse sequence: $CP-t_1-\pi/2-\tau-\pi/2-t_2$ where CP corresponds to $^{1}H-^{13}C$ cross polarization, t_1 was the evolution period, the first $\pi/2$ pulse rotated ^{13}C transverse magnetization to the longitudinal axis, τ was a spin diffusion period during which ^{13}C longitudinal magnetization was transferred between ^{13}C nuclei, the second $\pi/2$ pulse rotated ^{13}C longitudinal magnetization to the transverse plane, and t_2 was the detection period. Continuous-wave ^{1}H decoupling at 100 kHz was applied during the $\pi/2$ pulses, t_1, and t_2, but not during τ. The U-NAL setup compound was used to optimize all of the ^{1}H and ^{13}C rf fields with the ^{13}C $\pi/2$ pulse length set as half the π pulse length determined from a CP z-filter sequence.[58]

The following parameters were typical for the HFP-U3, HFP-U12, and IFP-U10 PDSD data acquisition: 44–64 kHz ramp on the ^{13}C CP rf field, 62.5 kHz ^{1}H CP rf field, 2 ms CP contact time, 50 kHz ^{13}C $\pi/2$ pulse rf field, 200 t_1 points with 25 μs dwell time, 1024 t_2 points with 20 μs dwell time, 1 s recycle delay, 1024 transients per free induction decay (FID), and 4.5 day total acquisition time. For each sample, a spectrum was taken with $\tau=10$ ms, and for the HFP-U3 and IFP-U10 samples a second spectrum was taken with $\tau=100$ ms. Hypercomplex data were obtained by acquiring two individual FIDs for each t_1 point with either a ^{13}C $(\pi/2)_x$ or $(\pi/2)_y$ pulse at the end of the t_1 evolution period. For the first of these t_1 FIDs, individual transients were coadded with the following phase cycling scheme: first ^{13}C $\pi/2$ pulse, $x, -x, x, -x, x, -x, x, -x$; second ^{13}C $\pi/2$ pulse, $x, x, y, y, -x, -x, -y, -y$; receiver, $y, -y, -x, x, -y, y, x, -x$. For the other t_1 FID, the first ^{13}C $\pi/2$ pulse followed $y, -y, y, -y, y, -y, y, -y$ cycling. The IFP PDSD data acquisition included a 41–59 kHz ramped ^{13}C CP rf field, 128 t_1 points, and 2048 transients per FID.

A $^{13}C-^{13}C$ spectrum of a HFP-U3 sample was obtained using a 16.4 T Bruker Advance spectrometer (Billerica, MA) and a triple resonance $^{1}H/^{13}C/^{15}N$ MAS probe equipped for use with 4 mm diameter rotors. The acquisition parameters included 176.065 (^{13}C) and 700.1 MHz (^{1}H) frequencies, 10 kHz MAS frequency, 67 kHz ^{13}C CP rf field, 77 kHz ^{1}H CP rf field, 2 ms CP contact time, 110 kHz SPINAL-64 ^{1}H decoupling, 64 t_1 points with 28.4 μs dwell time, $\tau=100$ ms, 444 t_2 points with 28.4 μs dwell time, 1 s recycle delay, 512 transients per FID, and ~1 day total acquisition time.[59]

Data were processed according to the method of states using NMRPIPE software.[60,61] Processing included zero filling, line broadening, and base line correction. The lowest contour level in a 2D plot was chosen at the largest positive extremum of the noise and the ratio of intensities between successive contours was chosen so that adjacent contours could be clearly viewed and peaks clearly distinguished.

2D $^{15}N-^{13}C$ experimental details

The 2D $^{15}N-^{13}C$ correlation experiments were acquired at 9.4 T with the probe in triple resonance $^{1}H/^{13}C/^{15}N$ configuration. Correlations were generated with the double cross polarization sequence: $CP1-t_1-CP2-t_2$ where CP1 corresponds to ^{1}H to ^{15}N cross polarization, t_1 was the evolution period, CP2 corresponds to selective $^{15}N-^{13}CO$ (NCO) or $^{15}N-^{13}C\alpha$ (NCA) cross polarization, and t_2 was the detection period.[62] Two-pulse phase modulation (TPPM) ^{1}H decoupling at 100 kHz was applied during the t_2 period, and continuous-wave decoupling was applied during the CP2 and t_1 periods.[63] The ^{1}H, ^{13}C, and ^{15}N rf fields were first optimized with U-NAL and the ^{15}N and ^{13}C rf fields during the CP2 step were then further optimized with the I4-U2 peptide.

For each sample, NCO and NCA spectra were obtained. The NCO acquisition parameters included 36–47 kHz ramp on the ^{15}N CP1 rf field, 57 kHz ^{1}H CP1 rf field, 1.1 ms CP1 contact time, 25 kHz ^{15}N CP2 rf field, 28 kHz ^{13}C CP2 rf field with the ^{13}C transmitter at ~155 ppm, 1.3 ms CP2 contact time, 41 t_1 points with 250 μs dwell time, 1024 t_2 points with 20 μs dwell time, 1 s recycle delay, and the ^{15}N transmitter at ~100 ppm. Hypercomplex data were collected by acquiring two FIDs for each t_1 point with either $^{15}N(CP2)_x$ or $^{15}N(CP2)_y$ phases. The following phase cycling scheme was used: ^{1}H $\pi/2$ $x,x,x,x,-x,-x,-x,-x$; ^{15}N CP1 x,x,x,x,x,x,x,x; ^{1}H CP1 y,y,y,y,y,y,y,y; ^{15}N CP2, x,x,x,x,x,x,x,x; ^{13}C CP2, $y,-x,-y,x,y,-x,-y,x$; receiver, $y,-x,-y,x,-y,x,y,-x$. For the other t_1 FID, the ^{15}N CP2 phase followed y,y,y,y,y,y,y,y. Each final data set was the sum of several individual complete t_1,t_2 sets which were each acquired with 1024 transients per FID and ~1 day signal averaging time. The NCA parameters were similar to the NCO parameters except for a 2.3 ms CP2 contact time, 29 kHz ^{13}C CP2 rf field, and a ^{13}C transmitter of ~35 ppm. Data were processed with NMRPIPE in a manner similar to that used for the 2D $^{13}C-^{13}C$ PDSD data.

RESULTS

HFP-U3

Figure 1 displays a 2D $^{13}C-^{13}C$ correlation spectrum for the HFP-U3 sample, with magnetization exchange driven by PDSD with $\tau=10$ ms. Only intraresidue crosspeaks were observed in this spectrum whereas sequential interresidue crosspeaks could be observed in the PDSD spectrum with $\tau=100$ ms.

Figure 2 displays 2D NCO and NCA correlation spectra for the HFP-U3 sample. In these spectra, crosspeaks between directly bonded $^{15}N-^{13}CO$ and $^{15}N-^{13}C\alpha$ nuclei were observed. The combination of the $^{13}C-^{13}C$ and $^{15}N-^{13}C$ spectra made possible a nearly unambiguous assignment of ^{13}C and ^{15}N nuclei in the three residues, as listed in Table I. The assignment relied on comparison of $^{15}N-^{13}C$ and intraresidue $^{13}C-^{13}C$ crosspeak shifts with characteristic ^{13}C and ^{15}N shifts of each residue type.[64] The shifts listed in Table I were obtained from the following sources: (1) ^{13}C sidechain and Gly ^{13}CO shifts from the $^{13}C-^{13}C$ spectra; (2) Phe ^{13}CO and ^{15}N shifts from the NCO and NCA spectra; and (3) Gly $^{13}C\alpha$, Phe $^{13}C\alpha$, Leu $^{13}C\alpha$, and Leu ^{13}CO shifts from all

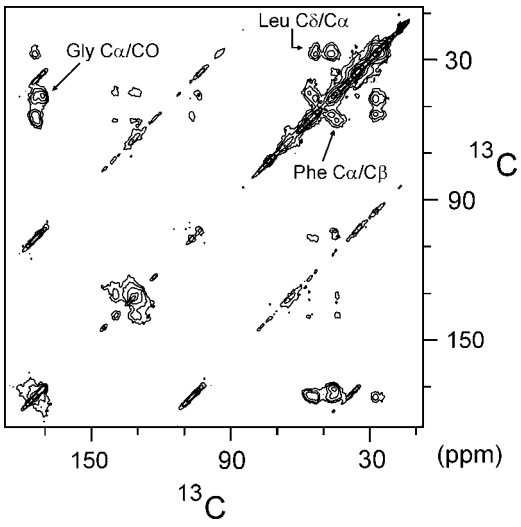

FIG. 1. 2D $^{13}C-^{13}C$ PDSD spectrum of HFP-U3 associated with LM3 membranes. The peptide:lipid molar ratio was ~0.04 with ~0.8 μmol HFP-U3. The sample pH was 7.0 and the sample volume in the 4 mm rotor was ~30 μl. The data were collected with 10 ms exchange time and total signal averaging time of ~4.5 days. The MAS frequency was 6.8 kHz. The spectrum was processed with 20 Hz Lorentzian line narrowing and 80 Hz Gaussian line broadening in the t_2 dimension and a sine+60° window in the t_1 dimension. The number of t_1 points was doubled by linear prediction. Adjacent contours have intensities which differ by a factor of 2.5. Some of the peak assignments are shown using the convention of assignment in f_1 (vertical axis)/ assignment in f_2 (horizontal axis).

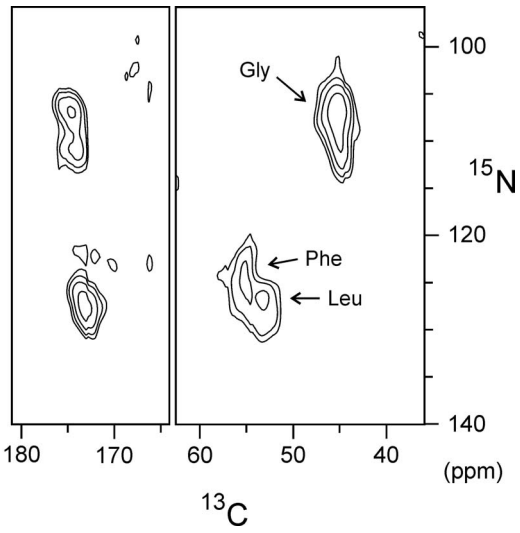

FIG. 2. 2D NCO (left) and NCA (right) spectra of HFP-U3 associated with LM3 membranes using the same sample as in Fig. 1. The MAS frequency was 7.0 kHz and the total signal averaging time for each spectrum was ~3 days. The spectra were processed with 100 Hz Gaussian line broadening in the ^{15}N dimension and 150 Hz Gaussian line broadening in the ^{13}C dimension. Adjacent contours have intensities which differ by a factor of 1.5. The NCO spectrum correlates $^{15}N_i/^{13}CO_{i-1}$ nuclei and the NCA spectrum correlates $^{15}N_i/^{13}C\alpha_i$ nuclei. Some of the peak assignments are shown.

relevant peaks in both the $^{13}C-^{13}C$ and the $^{15}N-^{13}C$ spectra. When averages were taken, all peaks were equally weighted. For a given nucleus, the typical variation in shift between different spectra was ~0.3 ppm and the largest variation was 0.85 ppm. Comparison of peak shifts in spectra processed with different parameters (e.g., phase) also showed ~0.3 ppm shift variation.

There are well-known correlations between Cα, Cβ, and CO shifts and local conformation. Figure 3 presents the differences between the experimental ^{13}C shifts and characteristic helical or β strand shifts.[45] The experimental chemical shifts were more consistent with β strand conformation. An interesting feature of the NCO and NCA spectra was the range of Gly-10 ^{15}N chemical shifts. For each spectrum, two peaks with Gly-10 ^{15}N shifts that were separated by 4.2 ppm in the ^{15}N dimension and by ~0.5 ppm in the ^{13}C dimension were observed. The ^{13}C secondary shifts suggested that all crosspeaks corresponded to β strand conformation. One possible assignment of the shift doubling is distinct populations of parallel and antiparallel strand arrangements. This hypothesis is consistent with a previous rotational-echo double resonance (REDOR) study showing a mixture of parallel and antiparallel strand arrangements.[27]

HFP-U12

Figure 4 displays a 2D $^{13}C-^{13}C$ correlation spectrum of HFP-U12 associated with LM3 membranes. Overlap in the $^{13}C-^{13}C$ spectrum was such that only amino acid-type assignment was possible, as listed in Table II.

Figure 5 displays 2D NCO (left) and NCA (right) correlation spectra for the HFP-U12 sample. The NCO spectrum displays two groups of crosspeaks. The group with upfield ^{15}N shifts corresponded to crosspeaks with $^{15}N/^{13}CO$ identities of G10/L9, G13/L12, and G16/A15, and the group with downfield ^{15}N shifts was a superposition of crosspeaks from the other eight $^{15}N/^{13}CO$ pairs in the peptide. The downfield ^{15}N region contained four resolvable peaks: (1) f_1, f_2 =122.0, 174.3 ppm, the upper left prominent peak; (2) 123.1, 171.1 and 121.4, 170.4 ppm, the two overlapped peaks at the upper right; and (3) 125.4, 172.9 ppm, weaker and toward the lower center left. The 122.0, 174.3 peak had a ^{13}CO shift which was close to the Ala and Leu shifts derived from the $^{13}C-^{13}C$ spectrum of this sample. The 123.1, 171.1 and 121.4, 170.4 ppm peaks had ^{13}CO shifts which were close to the Gly shift from the $^{13}C-^{13}C$ spectrum. The 125.4, 172.9 ppm peak had a ^{13}CO shift which was close to the Phe-8 shift of the HFP-U3 sample. Additional evidence for this Phe ^{13}CO assignment was spectral intensity at this shift in the $^{13}CO/Phe\text{-}^{13}C\alpha$ region of the $^{13}C-^{13}C$ spectrum of

TABLE I. ^{13}C and ^{15}N chemical shift assignments in ppm for the HFP-U3 sample.

	Cα	Cβ	Cγ	Cδ	C1	C2-C6	CO	N
Phe-8	55.8	44.1			139.1	131.7	173.0	125.0
Leu-9	53.4	46.8	27.5	24.9			174.3	127.2
Gly-10	45.3						171.0	107.0 111.2

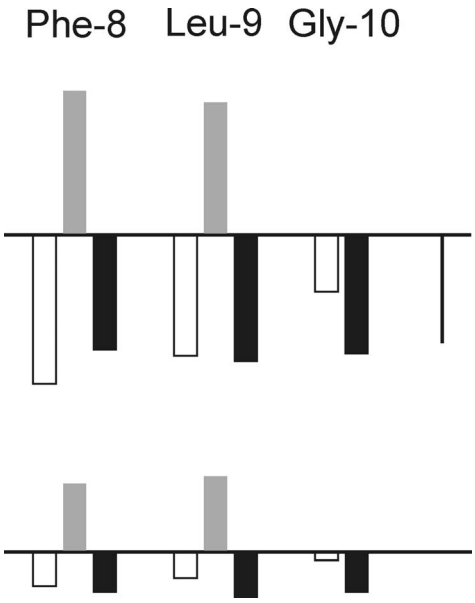

FIG. 3. Bar graphs for the HFP-U3 sample which display the differences between the experimentally derived ^{13}C shifts and characteristic helical (top) or β strand (bottom) ^{13}C shifts. The experimental shifts are reported in Table I and the characteristic helical and β strand shifts were obtained from reference tables (Ref. 45). The color code of the bars is Cα, white; Cβ, gray; and CO, black. The horizontal lines represent 0 ppm shift difference and the vertical bar at right represents the magnitude of a 5 ppm difference. In cases of two experimental shifts for a single nucleus, the bar value was calculated using the average shift. The experimental shifts of the HFP-U3 sample agree more closely with β strand shifts than with helical shifts.

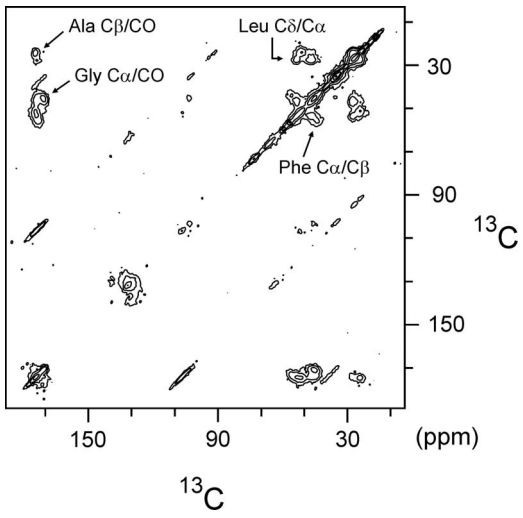

FIG. 4. 2D ^{13}C–^{13}C PDSD spectrum of HFP-U12 associated with LM3 membranes. The peptide:lipid molar ratio was ~0.04, the sample *p*H was 7.0, and the sample volume in the 4 mm rotor was ~30 μl with ~0.8 μmol HFP-U12. The data were collected with 10 ms exchange time and total signal averaging time of ~4.5 days. The MAS frequency was 6.8 kHz. The spectrum was processed with 80 Hz Gaussian line broadening in the t_2 dimension and a sine+60° window in the t_1 dimension. The number of t_1 points was doubled by linear prediction. Adjacent contours have intensities which differ by a factor of 2.8. Some of the peak assignments are shown using the convention of assignment in f_1 (vertical axis)/ assignment in f_2 (horizontal axis).

the HFP-U12 sample. Consideration of sequential ^{15}N–^{13}CO pairs with non-Gly ^{15}N resulted in the following assignments: (1) Upper left peak at 122.0, 174.3 ppm, ^{15}N/^{13}CO =A15/A14 and F8/L7; (2) upper right peaks at 123.1, 171.1 and 121.4, 170.4 ppm, A6/G5, A14/G13, and F11/G10; and (3) center-lower left peak at 125.4, 172.9 ppm, L9/F8 and L12/F11. Inclusion of the L9/F8 pair in assignment 3 was generally consistent with the shifts of the unambiguous L9/F8 assignment of the HFP-U3 sample. There was also spectral intensity in the 126, 174 ppm region which could be due to the L7/A6 pair.

In the NCA spectrum, there were two groups of crosspeaks, which could generally be assigned to Gly (upper right) and non-Gly (lower left) residues. The Gly ^{15}N intensity spanned 8 ppm and there were two peaks separated by 4.2 ppm, as in the HFP-U3 sample. In Table II, all of the ^{13}C shifts except for Gly ^{13}Cα were derived from analysis of the 2D ^{13}C–^{13}C spectra, and the ^{15}N shifts were derived from analysis of the NCO and NCA spectra. The Gly ^{13}Cα shift was the average of peak shifts in the ^{13}C–^{13}C and NCA spectra.

Figure 6 displays differences between the experimental ^{13}C shifts of the HFP-U12 sample and characteristic helical or β strand ^{13}C shifts. There was better agreement with the β strand shifts.

IFP-U10

Figure 7(a) displays a 2D ^{13}C–^{13}C correlation spectrum of IFP-U10 associated with PC/PG membranes. Spectral overlap was such that only amino acid-type assignment was possible, as listed in Table III. All the ^{13}C chemical shifts were obtained from the spectrum of Fig. 7.

As displayed in Fig. 7(b), four Gly ^{13}Cα/^{13}CO crosspeaks were observed. Peak A had ^{13}Cα and ^{13}CO shifts closer to those expected in helical conformation, peak B had ^{13}Cα and ^{13}CO shifts closer to those expected in β strand conformation, peak C had a ^{13}Cα shift closer to helical conformation and a ^{13}CO shift closer to β strand conformation, and peak D had a ^{13}Cα shift closer to β strand conformation and a ^{13}CO shift closer to helical conformation. The ratio of intensities of crosspeaks A:B:C:D was ~2:1.5:1:1 and the most intense crosspeaks were those with either purely helical (peak A) or purely β strand (peak B) secondary chemical

TABLE II. ^{13}C and ^{15}N chemical shift assignments in ppm for the HFP-U12 sample.

	Cα	Cβ	Cγ	Cδ	C1	C2-C6	CO	N
Ala	51.1	24.1					174.6	
Gly	45.4						170.8	106.6 110.8
Leu	53.3	46.9	27.4	23.8			174.1	
Phe	55.8	43.9			139.6	131.8		

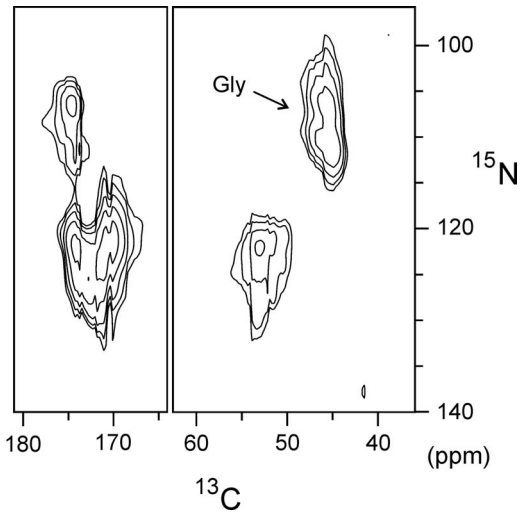

FIG. 5. 2D NCO (left) and NCA (right) spectra of HFP-U12 associated with LM3 membranes using the same sample as in Fig. 4. The MAS frequency was 7.0 kHz. Signal averaging times were ~5 and ~4 days for the NCO and NCA spectra, respectively. Spectra were processed using 100 Hz Gaussian line broadening in the ^{15}N dimension and 150 Hz Gaussian line broadening in the ^{13}C dimension. Adjacent contours have intensities which differ by a factor of 1.5. In the two spectra, the regions with upfield ^{15}N shifts include peaks which correlated with ^{15}N from Gly residues and the regions with downfield ^{15}N shifts include peaks which correlated with ^{15}N from non-Gly residues.

shifts. For the Ala, Ile, Leu, and Phe residues, only one crosspeak for each correlation type (e.g., $^{13}C\alpha/^{13}CO$) was clearly detected. More definitive (beyond residue-type) assignment was not obtained from analysis of $^{13}C-^{13}C$ spectra with $\tau=100$ ms (not shown) because of overlap between interresidue crosspeaks.

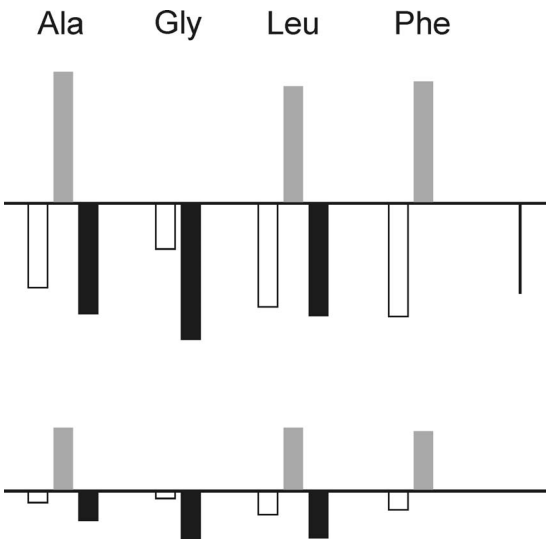

FIG. 6. Bar graphs for the HFP-U12 sample which display the differences between the experimentally derived ^{13}C shifts and characteristic helical (top) or β strand (bottom) ^{13}C shifts. The experimental shifts are reported in Table II and the characteristic helical and β strand shifts were obtained from reference tables (Ref. 45). The color code of the bars is Cα, white; Cβ, gray; and CO, black. The horizontal lines represent 0 ppm shift difference and the vertical bar at right represents the magnitude of a 5 ppm difference. In cases of two experimental shifts for a single nucleus, the bar value was calculated using the average shift. The experimental shifts of the HFP-U12 sample agree more closely with β strand shifts than with helical shifts.

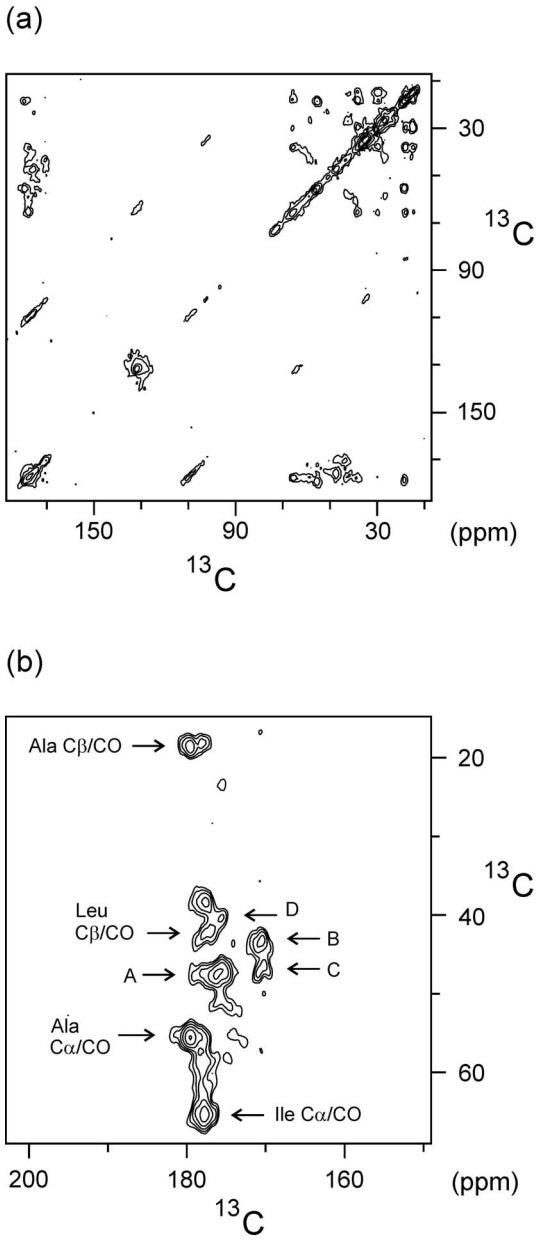

FIG. 7. 2D $^{13}C-^{13}C$ PDSD spectra with 10 ms exchange time of IFP-U10 associated with PC/PG membranes. Spectrum b is an expanded view of part of spectrum a. The peptide:lipid molar ratio was ~0.02, the sample pH was 5.0, and the sample volume in the 4 mm rotor was ~30 μl with ~0.3 μmol of IFP-U10. The MAS frequency was 6.8 kHz and the total signal averaging time was ~3 days. Spectra were processed with 80 Hz Gaussian line broadening in the t_2 dimension and a sine+60° window in the t_1 dimension. The number of t_1 points was doubled by linear prediction. Adjacent contours have intensities which differ by a factor of (a) 2.55 or (b) 1.4. Some of the peak assignments are shown using the convention of assignment in f_1 (vertical axis)/ assignment in f_2 (horizontal axis). The A, B, C, and D labels in spectrum b point to Gly Cα/CO crosspeaks.

Previous work on selectively Leu-2 ^{13}CO/Phe-3 ^{15}N labeled IFP associated with PC/PG membranes yielded a Leu-2 ^{13}CO shift of 177.7 ppm.[21] This was close to the 177.5 ppm shift determined from analysis of the spectra of Fig. 7 and provided evidence that the spectrum was assigned correctly.

Figure 8 displays 2D NCO (left) and NCA (right) correlation spectra of the IFP-U10 sample. In the NCA spectrum, the two largest crosspeaks were at 122.0, 55.3 and 105.8,

TABLE III. ^{13}C and ^{15}N chemical shift assignments in ppm for the IFP-U10 sample.

	Cα	Cβ	Cγ	Cδ	C2-C6	CO	N
Ala	55.5	18.6				179.4	122.0
Gly	47.4					175.9	105.8
	43.6					170.6	
	46.4					170.0	
	41.0					176.1	
Ile	65.6	38.1	29.6,18.0	14.7		177.8	
Leu-2	58.7	42.4	26.7	15.6		177.5	
Phe	60.5	39.7			131.8		

46.8 ppm. Using the $^{13}C\alpha$ shifts from the $^{13}C-^{13}C$ spectra, the most reasonable assignment of the crosspeaks was Ala and Gly, respectively, and the ^{15}N shifts listed in Table III were based on this assignment. The NCO spectrum had three distinct crosspeaks at f_1, f_2=120.4, 177.6; 123.3, 175.7; and 125.0, 169.7 ppm. Assignment was done using ^{13}CO shifts derived from the $^{13}C-^{13}C$ spectra and knowledge that Gly ^{15}N shifts are in the 100–115 ppm range. The most intense 120.4, 177.6 ppm peak was assigned to the I10/F9, A7/I6, and F3/L2 $^{15}N-^{13}CO$ sequential pairs. The 123.3, 175.7 and 125.0, 169.7 ppm peaks were assigned to the A5/G4, F9/G8, and L2/G1 pairs. The ^{13}CO shifts of these latter two peaks corresponded to helical and β strand Gly shifts, respectively. In addition to resonance overlap, the IFP-U10 NCO and NCA spectra had low signal-to-noise ratio and it was not possible to make more definitive ^{15}N shift assignments.

Figure 9 displays differences between the experimental ^{13}C shifts of the dominant crosspeaks in the IFP-U10 sample and characteristic helical or β strand ^{13}C shifts. There was better agreement with the helical shifts.

Comparative 9.4 and 16.4 T spectra

Figure 10 displays comparative 2D $^{13}C-^{13}C$ spectra of the HFP-U3/LM3 sample taken on a 9.4 (left) or 16.4 T (right) spectrometer. The 16.4 T spectrometer was located at Bruker, Inc. in Billerica, MA. Relative to 9.4 T, the ppm linewidths of the 16.4 T spectrum were narrower by a factor of ~0.6. For the Leu-9 $^{13}C\beta/^{13}C\alpha$ and $^{13}C\gamma/^{13}C\alpha$ crosspeaks in the 16.4 T spectrum, the Leu-9 $^{13}C\alpha$ linewidth in the f_2 dimension was ~1.4 ppm. Although the reduction in linewidth with increased field is not yet well understood, one contribution is attenuation of the $^{13}C-^{13}C$ scalar and dipolar couplings at the higher field.[65] Because of this favorable linewidth effect, assignment of membrane-associated FPs with U-^{13}C, ^{15}N labeling will likely be more straightforward at higher field.

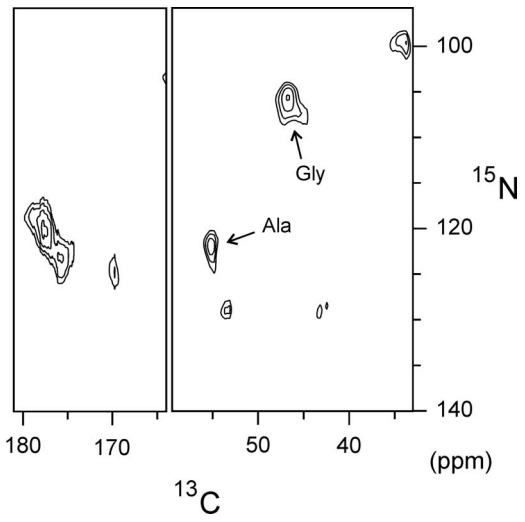

FIG. 8. 2D NCO (left) and NCA (right) spectra of IFP-U10 associated with PC/PG membranes using the same sample as in Fig. 7. The MAS frequency was 7 kHz. Signal averaging times were ~10 and ~4 days for NCO and NCA spectra, respectively. Both spectra were processed using 100 Hz Gaussian line broadening in the ^{15}N dimension and 150 Hz Gaussian line broadening in the ^{13}C dimension. Adjacent contours have intensities which differ by a factor of 1.25.

DISCUSSION

Assignments and secondary structure

The HFP-U3 sample was an example of scatter-uniform FP labeling and nearly unambiguous assignment was possible from 2D $^{13}C-^{13}C$ and $^{15}N-^{13}C$ spectra obtained on a 9.4 T spectrometer. The HFP-U12 and IFP-U10 samples were examples of more extensive FP labeling and only amino acid-type assignment was possible. The chemical shifts suggested that the HFP-U12 sample had predominant

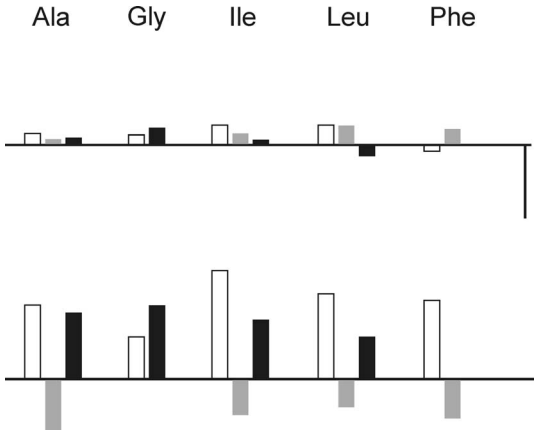

FIG. 9. Bar graphs for the IFP-U10 sample which display the differences between the experimentally derived ^{13}C shifts and characteristic helical (top) or β strand (bottom) ^{13}C shifts. The experimental shifts are reported in Table III and for Ala and Gly nuclei, the bar values were calculated with the shifts corresponding to the strongest crosspeaks. The characteristic helical and β strand shifts were obtained from reference tables (Ref. 45). The color code of the bars is Cα, white; Cβ, gray; and CO, black. The horizontal lines represent 0 ppm shift difference and the vertical bar at right represents the magnitude of a 5 ppm difference. The experimental shifts of the strongest crosspeaks in the spectrum of the IFP-U10 sample agree more closely with helical shifts than with β strand shifts.

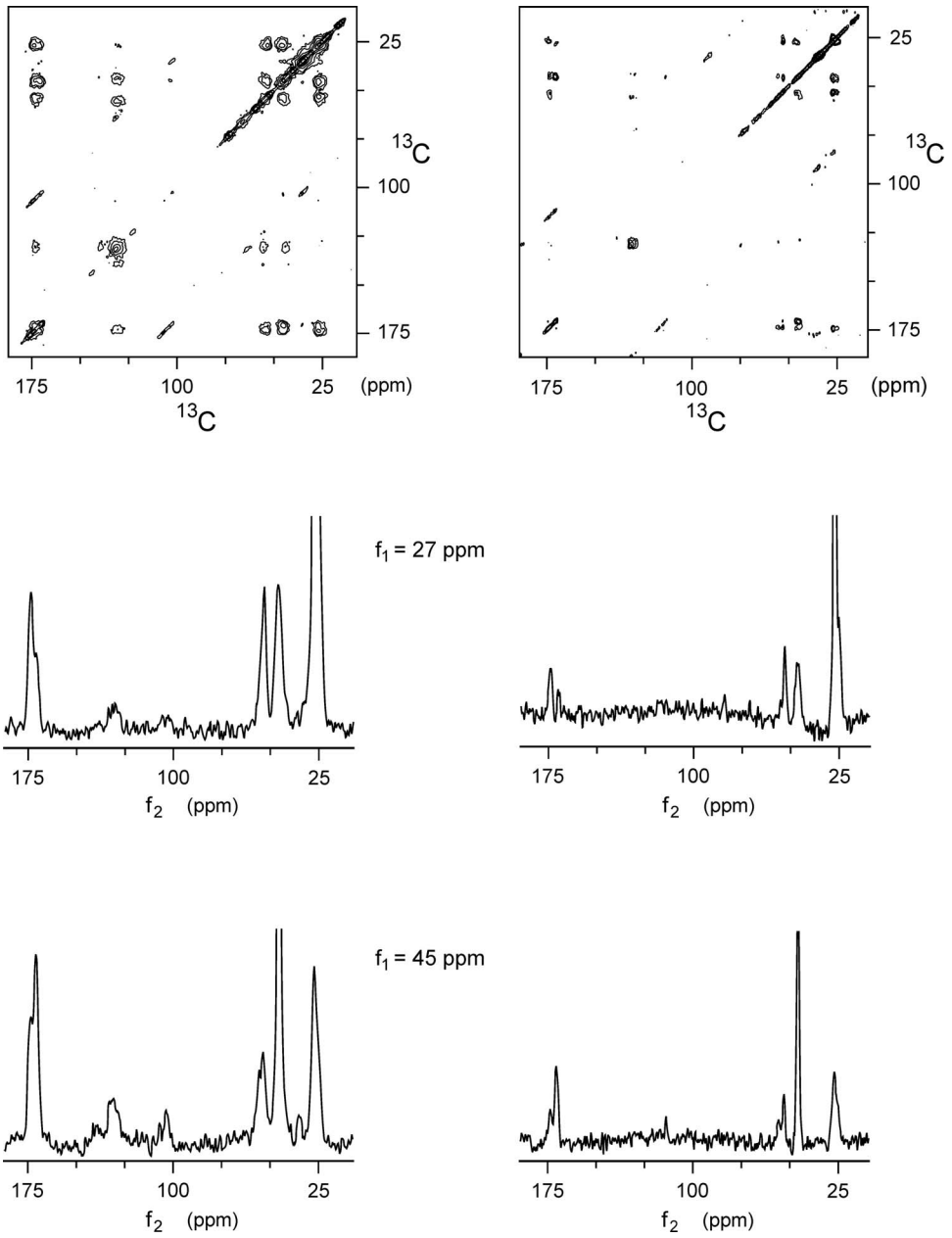

FIG. 10. 2D $^{13}C-^{13}C$ PDSD spectra of HFP-U3 associated with LM3 membranes obtained with either a 9.4 (left) or 16.4 T (right) spectrometer. The one-dimensional spectra display slices in the horizontal f_2 dimension for $f_1=27$ ppm and $f_1=45$ ppm. The peptide:lipid molar ratio was ~0.04 with ~0.8 μmol HFP-U3 and the exchange time was 100 ms. The 9.4 T spectrum was obtained with 6.8 kHz MAS frequency and with ~5 days signal averaging time and the 16.4 T spectrum was obtained with 10 kHz MAS frequency and with ~1 day signal averaging time. The 9.4 and 16.4 T spectra were, respectively, processed with 80 and 100 Hz Gaussian line broadening in the t_2 dimension. For both spectra, processing included linear prediction in the t_1 dimension that doubled the number of t_1 points and a sine+60° window in the t_1 dimension. Relative to 9.4 T, the ppm linewidths at 16.4 T are narrower by a factor of ~0.6. Some of the signal-to-noise difference between the two spectra may be due to different amounts of sample packed in the rotors.

β strand conformation over the labeled residues whereas the IFP-U10 sample had predominant helical conformation over the labeled residues. Unambiguous assignment has been achieved for U-^{13}C, ^{15}N labeled microcrystalline proteins of 50–110 residues. A significant difficulty for the membrane-associated FPs are larger linewidths (by a factor of ~25 in 2D crosspeak area). In this regard, the FP samples are similar to β-amyloid for which scatter-uniform labeling was necessary for a complete unambiguous assignment. The 16.4 T spectrum suggested that experiments at higher field may lead to improved resolution for FP samples.

Relative to microcrystalline proteins, the signals in the present study were reduced by broad linewidths and by the small but physiologically relevant amount of peptide in the sample volume. Because of lower signal, it was not feasible to obtain more information-rich 3D spectra. In future studies, signal intensity could be potentially augmented by (1) increasing the amount of peptide in the sample and concurrently reducing the amount of lipid and/or water, (2) working at higher field, and (3) using probes better suited for hydrated biological samples.[66]

The chemical shift-based dominant β strand conformation in the HFP-U12 sample and helical conformation in the IFP-U10 sample are consistent with previous solid-state NMR spectra of selectively labeled HFPs and IFPs as well as circular dichroism, infrared, and electron spin resonance spectra of the FPs.[13,21,49–51,67–69] The earlier solid-state NMR studies additionally suggested that the absence or presence of cholesterol in the membrane correlated with formation of helical or β strand conformation, respectively.[21,22] FP-induced fusion activity was observed for vesicles of either composition and suggests that both peptide conformations are fusogenic.[53]

The presence of multiple Gly ^{13}CO/$^{13}C\alpha$ crosspeaks in the IFP-U10 sample suggested that there were multiple conformations. This finding is consistent with infrared spectra

indicating populations of helical and β strand structure in PC/PG-associated IFPs.[70] The Gly $^{13}CO/^{13}C\alpha$ "peak C" in Fig. 7(b) was particularly intriguing because the $^{13}C\alpha$ shift was more characteristic of helical conformation while the ^{13}CO shift was more characteristic of β strand conformation. Studies on scatter-uniform labeled samples may be necessary to distinguish whether peak C was due to a single Gly residue with a unique conformation or to the same conformation appearing at multiple Gly residues. This is the only peptide in this study for which isotopic labeling extended to the N-terminus, and Gly-1 could be unstructured or atypically structured.

In both the HFP-U3 and HFP-U12 NCA spectra, each Gly $^{15}N-^{13}C\alpha$ region appeared to be a combination of two peaks which had ^{15}N shifts of ~107 and ~111 ppm. However, in the HFP-U3 spectrum, the 107 ppm peak was larger while in the HFP-U12 spectrum, the 111 ppm peak was larger. Quantitatively, the 107/111 intensity ratio was ~1.5 and ~0.9 in the HFP-U3 and HFP-U12 spectra, respectively. One hypothesis for assignment of the two shifts is parallel and antiparallel strand arrangements.[27] This may have significance for fusion because a parallel arrangement could lead to alignment of apolar N-terminal regions on adjacent strands and the resulting larger apolar volume could induce a larger local perturbation to membranes and a higher fusion rate. Cysteine cross-linked HFP induces a higher rate of membrane fusion than does non-cross-linked HFP and this difference might reasonably be ascribed to a higher fraction of parallel strand arrangement in the cross-linked HFP.[71] The Gly $^{15}N-^{13}C\alpha$ crosspeak intensities in spectra of cross-linked HFP-U12 may, therefore, provide insight into the relationship between ^{15}N shifts and strand arrangement in HFPs.

CONCLUSIONS

An amino acid-type ^{13}C, ^{15}N assignment was obtained for membrane-associated HFP and IFP with large contiguous regions of uniformly ^{13}C, ^{15}N labeled residues. The ^{13}C shifts of the dominant crosspeaks were consistent with predominant β strand conformation for HFP and helical conformation for IFP and this conformational difference may be partly ascribed to the presence and absence of cholesterol in the membranes of the HFP and IFP samples, respectively. For a HFP sample with more limited labeling, there were two ^{15}N shifts associated with Gly-10 which may be associated with different β strand arrangements such as parallel and antiparallel. Better resolved spectra were obtained at higher field and suggest that a combination of higher field and more limited labeling will be helpful in achieving unambiguous assignment for membrane-associated fusion peptides.

ACKNOWLEDGMENTS

This work was supported by NIH Award No. R01-AI47153. We acknowledge Robert Tycko, Aneta Petkova, Stanley Opella, Anna DeAngelis, Werner Maas, and Jim Frye for helpful discussions and for pulse programs.

[1] L. D. Hernandez, L. R. Hoffman, T. G. Wolfsberg, and J. M. White, Annu. Rev. Cell Dev. Biol. **12**, 627 (1996).
[2] D. M. Eckert and P. S. Kim, Annu. Rev. Biochem. **70**, 777 (2001).
[3] S. R. Durell, I. Martin, J. M. Ruysschaert, Y. Shai, and R. Blumenthal, Mol. Membr Biol. **14**, 97 (1997).
[4] R. M. Epand, Biochim. Biophys. Acta **1614**, 116 (2003).
[5] I. A. Wilson, J. J. Skehel, and D. C. Wiley, Nature (London) **289**, 366 (1981).
[6] C. M. Carr and P. S. Kim, Cell **73**, 823 (1993).
[7] K. Tan, J. Liu, J. Wang, S. Shen, and M. Lu, Proc. Natl. Acad. Sci. U.S.A. **94**, 12303 (1997).
[8] M. Caffrey, M. Cai, J. Kaufman, S. J. Stahl, P. T. Wingfield, D. G. Covell, A. M. Gronenborn, and G. M. Clore, EMBO J. **17**, 4572 (1998).
[9] J. Chen, J. J. Skehel, and D. C. Wiley, Proc. Natl. Acad. Sci. U.S.A. **96**, 8967 (1999).
[10] P. M. Colman and M. C. Lawrence, Nat. Rev. Mol. Cell Biol. **4**, 309 (2003).
[11] J. L. Nieva and A. Agirre, Biochim. Biophys. Acta **1614**, 104 (2003).
[12] P. V. Dubovskii, H. Li, S. Takahashi, A. S. Arseniev, and K. Akasaka, Protein Sci. **9**, 786 (2000).
[13] X. Han, J. H. Bushweller, D. S. Cafiso, and L. K. Tamm, Nat. Struct. Biol. **8**, 715 (2001).
[14] C. H. Hsu, S. H. Wu, D. K. Chang, and C. P. Chen, J. Biol. Chem. **277**, 22725 (2002).
[15] D. K. Chang, S. F. Cheng, and W. J. Chien, J. Virol. **71**, 6593 (1997).
[16] K. F. Morris, X. F. Gao, and T. C. Wong, Biochim. Biophys. Acta **1667**, 67 (2004).
[17] C. P. Jaroniec, J. D. Kaufman, S. J. Stahl, M. Viard, R. Blumenthal, P. T. Wingfield, and A. Bax, Biochemistry **44**, 16167 (2005).
[18] Y. L. Li and L. K. Tamm, Biophys. J. **93**, 876 (2007).
[19] C. M. Gabrys and D. P. Weliky, Biochim. Biophys. Acta **1768**, 3225 (2007).
[20] J. Yang, P. D. Parkanzky, M. L. Bodner, C. G. Duskin, and D. P. Weliky, J. Magn. Reson. **159**, 101 (2002).
[21] C. M. Wasniewski, P. D. Parkanzky, M. L. Bodner, and D. P. Weliky, Chem. Phys. Lipids **132**, 89 (2004).
[22] Z. Zheng, R. Yang, M. L. Bodner, and D. P. Weliky, Biochemistry **45**, 12960 (2006).
[23] H. J. Worman, T. A. Brasitus, P. K. Dudeja, H. A. Fozzard, and M. Field, Biochemistry **25**, 1549 (1986).
[24] R. C. Aloia, H. Tian, and F. C. Jensen, Proc. Natl. Acad. Sci. U.S.A. **90**, 5181 (1993).
[25] J. Zhang, A. Pekosz, and R. A. Lamb, J. Virol. **74**, 4634 (2000).
[26] B. Brugger, B. Glass, P. Haberkant, I. Leibrecht, F. T. Wieland, and H. G. Krasslich, Proc. Natl. Acad. Sci. U.S.A. **103**, 2641 (2006).
[27] J. Yang and D. P. Weliky, Biochemistry **42**, 11879 (2003).
[28] O. J. Murphy III, F. A. Kovacs, E. L. Sicard, and L. K. Thompson, Biochemistry **40**, 1358 (2001).
[29] A. Detken, E. H. Hardy, M. Ernst, M. Kainosho, T. Kawakami, S. Aimoto, and B. H. Meier, J. Biomol. NMR **20**, 203 (2001).
[30] C. P. Jaroniec, C. E. MacPhee, N. S. Astrof, C. M. Dobson, and R. G. Griffin, Proc. Natl. Acad. Sci. U.S.A. **99**, 16748 (2002).
[31] F. M. Marassi and S. J. Opella, Protein Sci. **12**, 403 (2003).
[32] A. Bockmann, A. Lange, A. Galinier, S. Luca, N. Giraud, M. Juy, H. Heise, R. Montserret, F. Penin, and M. Baldus, J. Biomol. NMR **27**, 323 (2003).
[33] W. T. Franks, D. H. Zhou, B. J. Wylie, B. G. Money, D. T. Graesser, H. L. Frericks, G. Sahota, and C. M. Rienstra, J. Am. Chem. Soc. **127**, 12291 (2005).
[34] D. Marulanda, M. L. Tasayco, M. Cataldi, V. Arriaran, and T. Polenova, J. Phys. Chem. B **109**, 18135 (2005).
[35] O. C. Andronesi, S. Becker, K. Seidel, H. Heise, H. S. Young, and M. Baldus, J. Am. Chem. Soc. **127**, 12965 (2005).
[36] R. Mani, M. Tang, X. Wu, J. J. Buffy, A. J. Waring, M. A. Sherman, and M. Hong, Biochemistry **45**, 8341 (2006).
[37] J. Pauli, M. Baldus, B. van Rossum, H. de Groot, and H. Oschkinat, ChemBioChem **2**, 272 (2001).
[38] F. Castellani, B. van Rossum, A. Diehl, M. Schubert, K. Rehbein, and H. Oschkinat, Nature (London) **420**, 98 (2002).
[39] T. I. Igumenova, A. J. Wand, and A. E. McDermott, J. Am. Chem. Soc. **126**, 5323 (2004).
[40] S. G. Zech, A. J. Wand, and A. E. McDermott, J. Am. Chem. Soc. **127**, 8618 (2005).
[41] A. T. Petkova, Y. Ishii, J. J. Balbach, O. N. Antzutkin, R. D. Leapman, F. Delaglio, and R. Tycko, Proc. Natl. Acad. Sci. U.S.A. **99**, 16742 (2002).

[42] S. Chimon and Y. Ishii, J. Am. Chem. Soc. **127**, 13472 (2005).
[43] A. T. Petkova, W. M. Yau, and R. Tycko, Biochemistry **45**, 498 (2006).
[44] S. Sharpe, W. M. Yau, and R. Tycko, Biochemistry **45**, 918 (2006).
[45] H. Y. Zhang, S. Neal, and D. S. Wishart, J. Biomol. NMR **25**, 173 (2003).
[46] C. D. Chang, M. Waki, M. Ahmad, J. Meienhofer, E. O. Lundell, and J. D. Haug, Int. J. Pept. Protein Res. **15**, 59 (1980).
[47] L. Lapatsanis, G. Milias, K. Froussios, and M. Kolovos, Synthesis **8**, 671 (1983).
[48] M. L. Bodner, Ph.D. dissertation, Michigan State University, 2006.
[49] X. Han and L. K. Tamm, Proc. Natl. Acad. Sci. U.S.A. **97**, 13097 (2000).
[50] J. Yang, C. M. Gabrys, and D. P. Weliky, Biochemistry **40**, 8126 (2001).
[51] J. C. Macosko, C. H. Kim, and Y. K. Shin, J. Mol. Biol. **267**, 1139 (1997).
[52] M. Caffrey, *LIPIDAT: A Database of Thermodynamic Data and Associated Information on Lipid Mesomorphic and Polymorphic Transitions* (CRC, Boca Raton, FL, 1993).
[53] P. D. Parkanzky, Ph.D. dissertation, Michigan State University, 2006.
[54] K. L. Williamson, *Macroscale and Microscale Organic Experiments*, 2nd ed. (Heath, Lexington, 1994).
[55] H. W. Long and R. Tycko, J. Am. Chem. Soc. **120**, 7039 (1998).
[56] C. R. Morcombe and K. W. Zilm, J. Magn. Reson. **162**, 479 (2003).
[57] J. L. Markley, A. Bax, Y. Arata, C. W. Hilbers, R. Kaptein, B. D. Sykes, P. E. Wright, and K. Wuthrich, Pure Appl. Chem. **70**, 117 (1998).
[58] M. L. Bodner, C. M. Gabrys, P. D. Parkanzky, J. Yang, C. A. Duskin, and D. P. Weliky, Magn. Reson. Chem. **42**, 187 (2004).
[59] B. M. Fung, A. K. Khitrin, and K. Ermolaev, J. Magn. Reson. **142**, 97 (2000).
[60] D. J. States, R. A. Haberkorn, and D. J. Ruben, J. Magn. Reson. **48**, 286 (1982).
[61] F. Delaglio, S. Grzesiek, G. W. Vuister, G. Zhu, J. Pfeifer, and A. Bax, J. Biomol. NMR **6**, 277 (1995).
[62] M. Baldus, A. T. Petkova, J. Herzfeld, and R. G. Griffin, Mol. Phys. **95**, 1197 (1998).
[63] A. E. Bennett, C. M. Rienstra, M. Auger, K. V. Lakshmi, and R. G. Griffin, J. Chem. Phys. **103**, 6951 (1995).
[64] J. N. S. Evans, *Biomolecular NMR Spectroscopy* (Oxford, New York, 1995).
[65] S. K. Straus, T. Bremi, and R. R. Ernst, Chem. Phys. Lett. **262**, 709 (1996).
[66] J. A. Stringer, C. E. Bronnimann, C. G. Mullen, D. H. H. Zhou, S. A. Stellfox, Y. Li, E. H. Williams, and C. M. Rienstra, J. Magn. Reson. **173**, 40 (2005).
[67] F. B. Pereira, F. M. Goni, A. Muga, and J. L. Nieva, Biophys. J. **73**, 1977 (1997).
[68] S. G. Peisajovich, R. F. Epand, M. Pritsker, Y. Shai, and R. M. Epand, Biochemistry **39**, 1826 (2000).
[69] M. E. Haque, V. Koppaka, P. H. Axelsen, and B. R. Lentz, Biophys. J. **89**, 3183 (2005).
[70] X. Han and L. K. Tamm, J. Mol. Biol. **304**, 953 (2000).
[71] R. Yang, M. Prorok, F. J. Castellino, and D. P. Weliky, J. Am. Chem. Soc. **126**, 14722 (2004).